# HELIOSPHERIC EVOLUTION OF THE HELIUM ISOTOPES

I. ROTH
*Space Sciences Laboratory, University of California, Berkeley, CA 94720, U.S.A.*

(Received 15 July 1996; accepted 15 August 1996)

**Abstract.** The isotopic ratio of $^3$He/ $^4$He, which is routinely measured in the solar wind, on meteorites and in different astrophysical environments, is confined to several times $10^{-4}$. However, in impulsive solar flares this ratio reaches often values larger than unity. The evolution of this ratio from the primordial nucleosynthesis to the present solar conditions is sketched and the resonant plasma effects which enhance spectacularly the abundance of $^3$He in the impulsive solar flares are described.

## 1. Introduction

The evolution of the heliospheric ion populations includes a variety of nuclear, atomic, and plasma processes. Changes in elemental abundances occur at several transport stages in the solar and heliospheric environment. Observations of energetic solar ions in the interplanetary space and particularly their anomalous elemental and isotopic ratios contribute significantly to our understanding of these evolutionary stages. Of particular interest are those processes in the solar environment which modify the ratios of photospheric or coronal ions. The photospheric data of elemental or isotopic abundances is obtained remotely via spectroscopic methods with thermodynamic modelling of the solar atmosphere (Anders and Grevesse, 1989), while the interplanetary measurements are performed *in situ* by Si detectors with the $\mathrm{d}E/\mathrm{d}x$ vs $\mathbf{E}$ (Mason *et al.*, 1986; von Rosevinge *et al.*, 1978) or time of flight (with the geomagnetic cutoff) method (Mason *et al.*, 1995).

X-ray observations indicate that solar flares can be characterized into two distinct classes: impulsive with durations of minutes and gradual with durations of hours or days (Wild, Smerd, and Weiss, 1963; Pallavicini, Serio, and Vaiana, 1977; Reames, 1990; Reames, Meyer, and Rosenvinge, 1994). Ion observations in interplanetary space at energies of MeV nucl$^{-1}$ distinguish these two classes by their substantially different ion ratios: coronal abundances in the gradual events vs enhancement in the impulsive flares of 3–4 orders of magnitude in the $^3$He/$^4$He ratio and up to one order of magnitude in heavy ions. These enhancements, particularly in the He isotopic ratio, constitute one of the largest enrichments in heliospheric physics and the time scales involved make it one of the most effective acceleration processes encountered in space physics.

In this paper, the different processes which affect the $^3$He/$^4$He ratio from the presolar epoch till the *in situ* observations by satellites are surveyed. These processes include nuclear physics interaction at the primordial plasma, long-term galactic evolution, transport from the solar photosphere to the corona and resonant wave-particle interaction in the impulsive solar flares.

*Solar Physics* **172:** 297–305, 1997.

## 2. Primordial and Galactic $^3$He/ $^4$He Ratio

When the expanding primordial Universe cools down to temperatures of $10^9$ K $\sim$100 keV, the neutrinos are decoupled from the nuclear matter and the neutron-proton equilibration via weak interations ceases ('freeze-out'). At this stage the interaction is controlled mainly by the strong nuclear reactions with well-known cross sections. Due to the bottlenecks of instability at nuclei with mass 5 and 8 and the stability of $^4$He, almost all the neutrons are converted into $^4$He and the resulting abundances include H and $^4$He with small traces of $^2$D, $^3$He, and $^7$Li. In homogeneous nucleosynthesis the abundances of all these light elements depend only on one parameter: the ratio of baryons to photons, $\eta = \eta_b/n_\gamma$. In the last 25 years the only modifications of these results were due to an improved value of neutron lifetime (889 s) and to the number of neutrino flavours which was confirmed as three. Since the primordial photon density at 2.7 K is known, the observed relative ratios between the light elements bound the values on baryon density, resulting in important conclusions about the existence of dark matter (e.g., Reeves, 1993).

The primordial abundance of $^4$He, which is derived from observed emissions in metal-poor extragalactic H II regions (Pagel *et al.*, 1982; Olive and Steigman, 1995) and absorption spectra of quasars with high redshift (Jakobsen *et al.*, 1994), in good agreement with the cosmological nucleosynthesis theory, is believed to be kept unchanged in the external layers of stars while being processed in their cores. The resulting cosmological value for the $^4$He mass fraction is 0.245. Similarly, $^3$He is formed in the primordial stage and is augmented in the pre-Main-Sequence phase of stellar nucleosynthesis mainly by the complete burning of the fragile $^2$H, with an additional production in low-mass stars, $1 < M/M_0 < 2.5$, and net destruction in massive stars $2.5 < M/M_0 < 100$, at the later stage (Dearborn *et al.*, 1986), such that $^3$He in the solar surface represents the upper limit of the (D+$^3$He) abundance in the protosolar gas (Geiss and Reeves, 1972; Geiss, 1993). The survival rate of $^3$He during the galactic evolution is assessed as more than 80% (Yang *et al.*, 1894). Since the meteoric $^3$He/$^4$He ratio in carbonaceous chondrites, which are not contaminated by the solar deuterium burning, is found to be $\sim 1.5 \times 10^{-4}$ (Eberhardt, 1974) and the best deuterium observations in the interstellar medium (e.g., Vidal-Madjar, 1991) and by the Hubble telescope (Linsky *et al.*, 1995) give D/$^4$He $= (1.5 \sim 2.5) \times 10^{-4}$, the deduced value for the solar $^3$He/$^4$He ratio becomes $\sim 4 \times 10^{-4}$. This value is consistent with the nucleosynthesis result for primordial abundances (Yang *et al.*, 1984), with the observations of hot, ionized gas clouds (Vangioni-Flam, Olive, and Prantzos, 1994), with solar photospheric values and with the solar wind.

## 3. Photospheric vs Coronal $^3$He/$^4$He Ratio

While the photospheric abundances are deduced remotely, the coronal abundance ratios can be assessed directly by comparison to the solar wind. Indirectly one may also obtain isotopic ratios utilizing different nuclear reactions due to flare-accelerated particles. The first measurements of the He isotopic ratio were obtained from foils exposed on the Moon by Apollo astronauts (Geiss and Reames, 1972) and on board the ISEE-3 satellite (Coplan *et al.*, 1984), with the best fit of $^3\text{He}/^4\text{He} = 4.4 \times 10^{-4}$. Solar flares which are activated due to relaxation of coronal magnetic energy, release copious numbers of particles which may be used also as probes of the chromospheric isotopic ratios. Since flare-accelerated neutrons can be captured in the solar photosphere radiatively by protons and nonradiatively by $^3$He nuclei, the time-dependent neutron-capture gamma-ray line at 2.2 MeV gives a sensitive measure of the solar $^3$He/H ratio (Hua and Lingenfelter, 1987). The best fits give a photospheric $^3$He/H ratio of $2 \times 10^{-5}$, close to the accepted galactic ratio.

Important abundance changes in the outer solar atmosphere occur during the transport of coronal ions from the photosphere by a charge-dependent mechanism, resulting in ion-neutral fractionation and in specific element enrichment in large active regions (Meyer, 1985, 1996; von Steiger *et al.*, 1995). The elements with a low first ionization potential (FIP) are enhanced by a factor of four vs high FIP elements. This process emphasizes the transport of gas consisting of a mixture of ions and neutrals in the presence of low temperature photospheric radiation. In the solar wind the $^4$He/H ratio is approximately 0.04, $\sim$2 times lower than in the photosphere. This effect may be due to the longer ionization time of He during the neutral-ion fractionation process. However, since the same atomic physics process applies to both He isotopes, the ratio $^3$He/$^4$He does not change during the transport between the photosphere and the corona.

## 4. Resonant Enhancement of the $^3$He/$^4$He Ratio

The existence of electromagnetic ion-cyclotron waves in conjungtion with fluxes of electrons is frequently confirmed in the terrestrial aurora. These intense electromagnetic hydrogen cyclotron waves were observed on board several satellites crossing the auroral acceleration regions: S3-3 (Gurnett and Frank, 1972; Lysak and Temerin, 1983), *Viking* (Gustafsson *et al.*, 1990), *Freja* (Erlandson *et al.*, 1994) and the recently launched Polar satellite with the ability to measure directly all three components of the electric field.

Figure 1 shows the perpendicular and the parallel components of the electric field as well as the three magnetic components in a spinning frame during a traversal of the acceleration region at the south pole. The perpendicular/parallel electric fields were obtained by determining the background magnetic field and performing the vector products with the observed electric data. From Figure 1 one

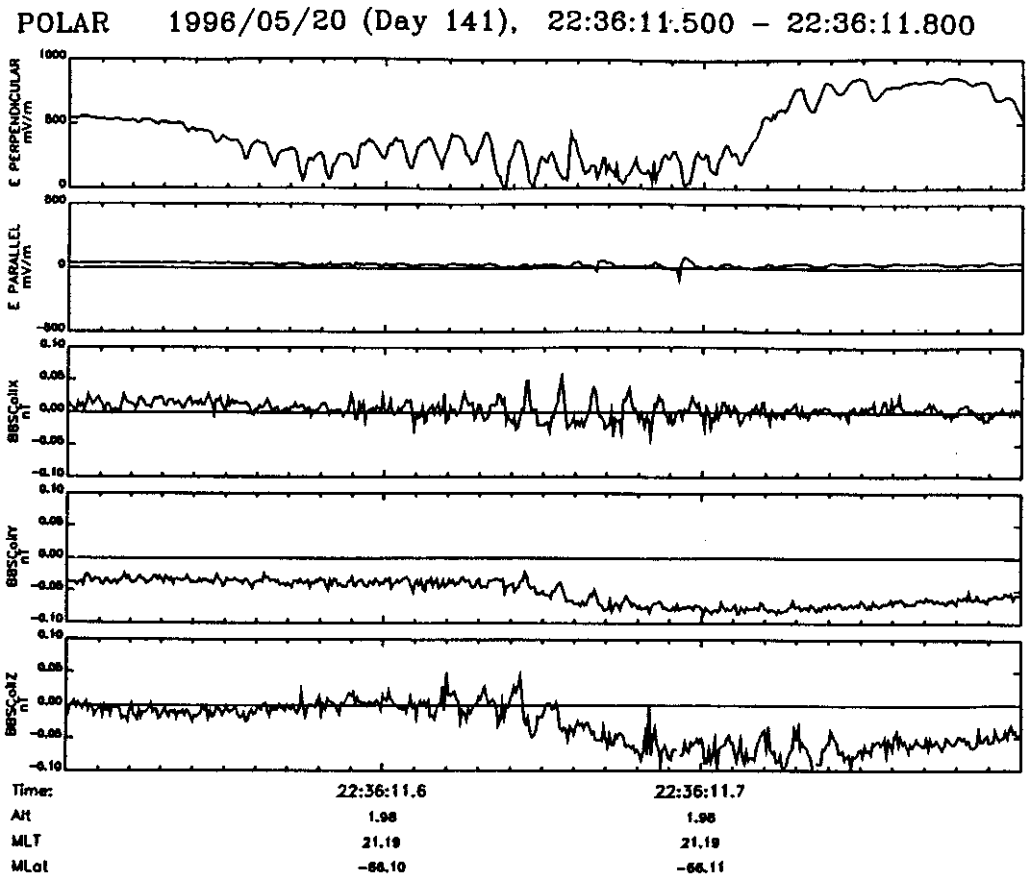


*Figure 1.* Perpendicular and parallel electric field components and three magnetic wave components as observed by the Polar satellite.

observes a long train of both electric and magnetic waveforms below 100 Hz, which are slightly below the hydrogen gyrofrequency. The measured fields indicate the existence of intense electromagnetic ion cyclotron wave fields at the acceleration region. Similar measurements are obtained at many crossings of the auroral zone close to the perigee of the orbit.

There exists an interesting analogy between physical processes on active auroral and flaring coronal field lines, as was suggested by Temerin and Roth (1992). Both environments consist of very low-$\beta$ plasmas, are dominated by two majority species, and due to magnetic field reconfigurations, are subjected to large electron fluxes. In the corona these electron fluxes are deduced from the X-ray emissions, while in the aurora they are measured directly by rockets or satellites. Therefore, it was argued that one can infer about coronal processes from the auroral *in situ* observations.

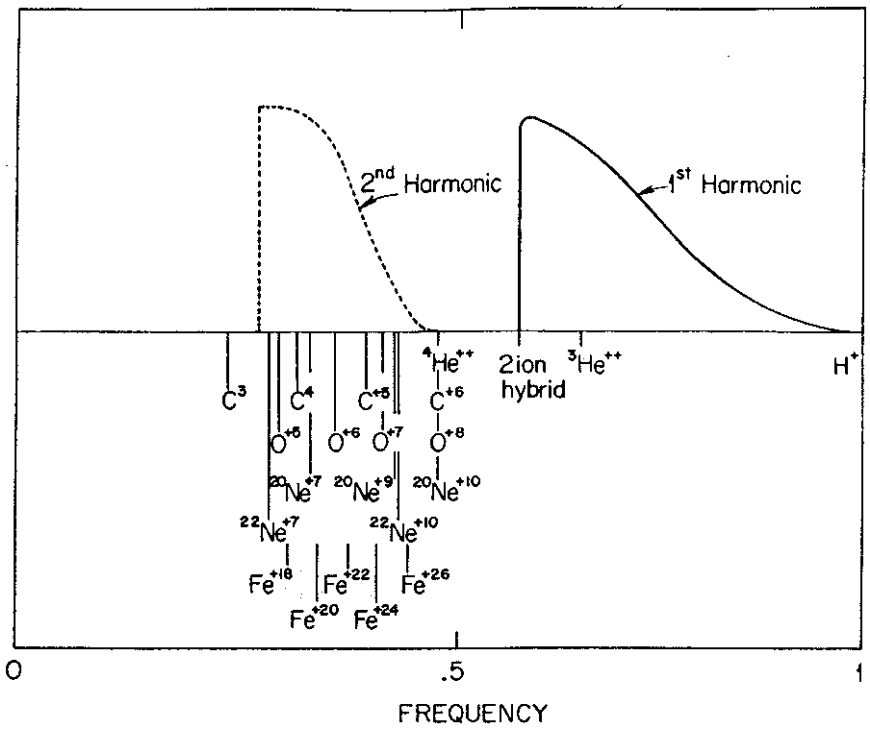


*Figure 2.* Schematic wave profile and partial configuration of the coronal ions.

The acceleration model is based on the resonant interaction with the parallel or obliquely propagating electromagnetic cyclotron waves. The frequency range of these waves is confined to below the hydrogen gyrofrequency and above the ion-hybrid frequency. $^3$He ions are unique among all the minority coronal ions in possessing a cyclotron frequency in that frequency range. When the wave which propagates along the inhomogeneous magnetic field passes through Doppler-shifted gyrofrequency of $^3$He these ions are resonantly accelerated, while the heavier ions are accelerated at the higher harmonic of their cyclotron frequency. The waves are dumped near the H and $^4$He gyrofrequencies; therefore ions with a charge-to-mass ratio of 0.5 (in units of H), like $^4$He or fully ionized CNO, are not affected by the waves. Figure 2 describes schematically the frequency range of the cyclotron waves with the configuration of several coronal ions as a function of their (normalized) gyrofrequencies.

The average parallel acceleration of a $^3$He ion gyrating in the combined stationary and monochromatic wave field with a gyrophase $\theta$ and a perpendicular velocity $v_\perp$ is given approximately by

$$m\frac{\mathrm{d}(\gamma v_\parallel)}{\mathrm{d}t} = q[(k_\parallel v_\perp/\omega)\hat{e}_\pm \cos(\phi_\pm) + (m\gamma v_\perp^2/2)\,\partial_z \ln B]\,, \tag{1}$$

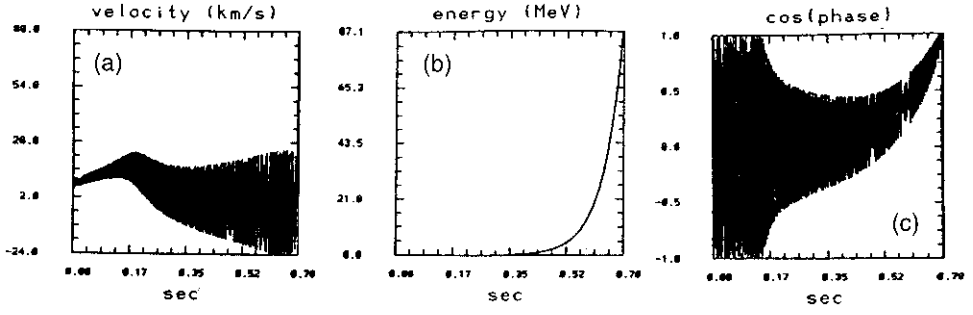


*Figure 3.* Solution of the model equations for parallel propagation. Density $n = 1.0 \times 10^9$, magnetic field $B = 400$ G, its gradient $L = 2000$ km. (a) Parallel velocity; (b) total energy; (c) $\cos\phi$.

where $e_\pm$ are the two circularly polarized electric components, $\phi_\pm = \theta \mp \psi$ denotes the angle between the wave phase and the ion gyrophase for each polarization, and the last term represents the mirror force. The energy equation is dominated at the resonance by the perpendicular contribution

$$\dot{W} = mc^2\dot{\gamma} = qv_\perp \hat{e}_\pm \cos\phi_\pm \,, \tag{2}$$

while the balance of perpedicular forces results in the phase equation

$$\dot{\phi}_\pm \sim (\Omega/\gamma) \pm (k_\parallel v_\parallel - \omega + k_\perp v_\perp \cos\theta) -$$
$$-\frac{q}{m}(\hat{e}_\pm \sin\phi_\pm / v_\perp \gamma)\,(1 - k_\parallel v_\parallel/\omega) \,, \tag{3}$$

where $\Omega(\mathbf{x})$ denotes the spatially-dependent gyrofrequency. For parallel propagation the polarizations are decoupled, while for highly oblique propagation both polarizations are of the same order. In the following we present a solution of the above set of equations together with an explicit particle simulation of $^3$He in the presence of an external field $\mathbf{B}_0 = B_0[(1 - z/L)\hat{\mathbf{z}} + (x\hat{x} + y\hat{y})/2L]$.

Figure 3 depicts the solution of the above equations for parallel propagation with the neglect of relativistic corrections. As the ion approaches the resonance, its perpendicular energy increases exponentially (Temerin and Roth, 1995), its average parallel motion slows down while the relative phase is bounded, indicating trapping. The phase factor $\cos\phi$ in the electromagnetic force (Equations (1) and (2)) which decelerates the parallel ion motion ($k_\parallel < 0$) and heats it perpendicularly, increases with time to compensate the increasing mirror force. When $\phi$ reaches $0^\circ$ the mirror force overcomes the wave force and expels the ion. The final ion energy for the chosen parameters is 87 MeV.

Figure 4 shows the results of full Lorentz $^3$He simulation for an obliquely propagating cyclotron wave. The effective force is now due to wave polarization and includes an additional factor $J_1(k_\perp\rho)/(k_\perp\rho)$ (Temerin and Roth, 1992) which

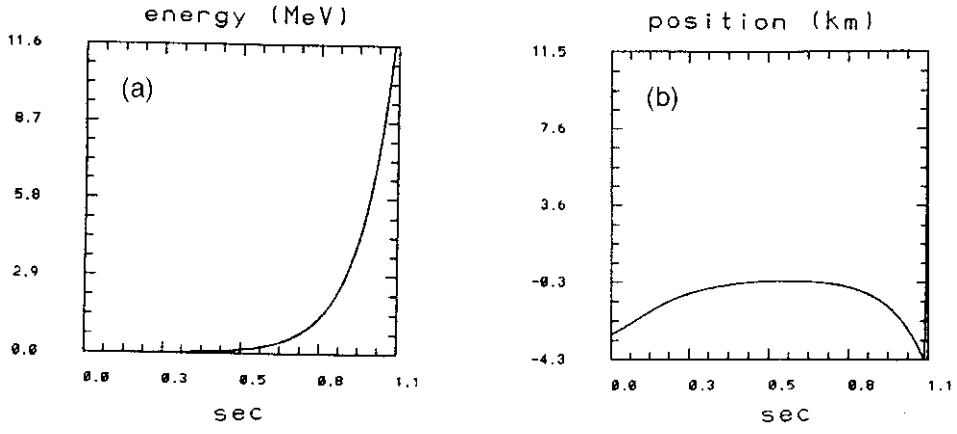


*Figure 4.* Solution of the Lorentz equations of motion for $^3$He with oblique propagation. $B = 500$ G, $n = 4.0 \times 10^9$, $L = 2000$ km, $k_\perp = 400$ km$^{-1}$. (a) Total energy; (b) parallel trajectory.

determines the final ion acceleration. Similarly to the parallel case the ion is slowed down in the parallel direction, while accelerated in the perpendicular. The reversal of ion motion (Figure 4(b)) is caused by a relativistic decrease of gyrofrequency which moves the resonance to a stronger magnetic field (Temerin and Roth, 1995). One observes that the $^3$He ion interacting with a wave at its gyrofrequncy can be accelerated to energy of several MeV in a fraction of second. This process affects all the $^3$He ions which reside in the flaring region, such that almost all of its $10^{31}$ $^3$He ions may be efficiently accelerated to energies of several MeV nucl$^{-1}$ and above (Reames, 1993). The result is a spectacular increase in the $^3$He/$^4$He ratio.

## 5. Conclusions

The evolution of the He isotopes follows a long journey from the primordial epoch till their observation in interplanetary space. The conditions during the first minutes of the primordial nucleosynthesis determine the isotopic ratio $^3$He/$^4$He $\sim 1.5 \times 10^{-4}$ as observed on the carbonaceous chondrites meteorites and at several primitive astrophysical objects. The main effect during the galactic chemical evolution is the almost complete burning of the fragile deuterium into $^3$He. Since most of the $^3$He survive stellar nucleosynthesis, the solar isotopic ratio settles around $4.1 \times 10^{-4}$. The transport from the photosphere to the corona decreases the ratio of He/H but does not affect the He isotopic ratio. The solar wind as well as energetic MeV ions which populate the heliosphere after gradual solar flares preserve this ratio. However, during the impulsive, electron-rich solar flares which are associated with large fluxes of electrons, and, by analogy to the terrestrial aurora, with intense electromagnetic ion-cyclotron waves, an efficient wave particle interaction takes place. Since the $^3$He ions are the only species which may satisfy the first harmonic

resonance condition with the cyclotron waves, they are accelerated to energies of several MeV nucl$^{-1}$ in a fraction of second. The effectiveness of this process allows all of the $^3$He ions which reside in the resonant region to be accelerated and ejected into interplanetary space. This process results in an increase of the He isotopic ratio, by several orders of magnitude, as observed by satellites in interplanetary space. The heliospheric $^3$He/$^4$He ratio, which accretes in oceanic sediments during the solar system epoch, is an important factor in determination of geological phenomena (Takayanagi and Ozima, 1987) and may be used as as a proxy of major glacial periods (Farley and Patterson, 1995).

## Acknowledgements

We acknowledge the support of NSF grant ATM 9224688 and NASA Polar grant NAG5–3182 and contract NAS5−30367.

## References

Anders, E. and Grevesse, H.: 1989, *Geochim. Cosmochim. Acta* **53**, 197.
Coplan, M. A., Oglivie, K. W., Bochder, P., and Geiss, J.: 1984, *Solar Phys.* **93**, 415.
Dearborn, D. S. P., Schramm, D. N., and Steigman, G.: 1986, *Astrophys. J.* **302**, 35.
Eberhardt, P.: 1974, *Earth PLanet. Sci Letters* **24**, 182.
Erlandsson, R. E., Zanetti, L. J., Acuna, M. H., Ericksson, A. I., Boehm, M. H., and Blomberg,L. G.: 1994, *Geophys. Res. Letters* **21**, 1885.
Farley, K. A. and Patterson, D. B.: 1995, *Nature* **378**, 600.
Geiss, J.: 1993, in N. Prantzos, E. Vangioni-Flam, and M. Casse (eds), *Origin and Evolution of Elements*, Cambridge University Press, Cambridge.
Geiss, J. and Reeves, H.: 1972, *Astron. Astrophys.* **18**, 126.
Gurnett, D. A. and Frank, L. A.: 1972, *J. Geophys. Res.* **77**, 3411.
Gustafsson, G., André, M., Matson, L., and Koskinen, H.: 1990, *J. Geophys. Res.* **95**, 5889.
Hua, X. M. and Lingenfelter, R. E.: 1987, *Astrophys. J.* **319**, 55.
Jakobsen, P., Boksenberg, A, Deharveng, J. M., Greenfield, P., Jedrzejewski, R., and Paresce, F.: 1994, *Nature* **370**, 35.
Linsky, J. L., Diplas, A., Wood, B. E., and Brown, A.: 1995, *Astrophys. J.* **451**, 335.
Lysak, R. L. and Temerin, M.: 1993, *Geophys. Res. Letters* **10**, 643.
Mason, G. M., Reames, D. V., Klecker, B., Hovestadt, D., and von Rosenvinge, T. T.: 1986, *Astrophys. J.* **303**, 849.
Mason, G. M., Reames, D. V., Klecker, B., Hovestadt, D., and von Rosenvinge, T. T.: 1995, *Astrophys. J.* **401**, 398.
Meyer, J. P.: 1985, *Astrophys. J. Suppl.* **67**, 173.
Meyer, J. P.: 1996, in S. S. Holland and G. Sonneborn (eds), 'Abundance Anomalies in the Solar Outer Atmosphere', *The Cosmic Abundances, ASP Conference Series* **99**, 127.
Olive, K. A. and Steigman, G.: 1995, *Astrophys. J. Suppl.* **97**, 49.
Pagel, B. E. J., Simonson, E. A., Terlevich, R. J., and Edmonds, M. G.: 1982, *Monthly Notices Roy. Astron. Soc.* **255**, 325.
Pallavicini, R., Serio, S., and Vaiana, G. S.: 1977, *Astrophys. J.* **216**, 108.
Reames, D. V.: 1990, *Astrophys. J.* **73**, 235.
Reames, D. V.: 1993, *Adv. Space Res.* **13**, 931.
Reames, D. V., Meyer, J. P., and von Rosenvinge, T. T.: 1994, *Astrophys. J. Suppl.* **90**, 649.

Reeves, H.: 1993, in N. Prantzos, E. Vangioni-Flam, and M. Casse (eds), 'The Saga of Light Elements', in *Origin and Evolution of the Elements*, Cambridge University Press, Cambridge.
Takayanagi, M. and Ozima, M.: 1987, *J. Geophys. Res.* **92**, 12531.
Temerin, M. and Roth, I.: 1996, in R. Ramaty, N. Mandzhavidze, and M. X. Hua (eds), *High Energy Solar Physics*, AIP Conference Proceedings, Greenbelt.
Temerin, M. and Roth, I.: 1992, *Astrophys. J.* **391**, L105.
Vangioni-Flam, E., Olive, K. A., Prantzos, N.: 1994, *Astrophys. J.* **427**, 618.
Vidal-Madjar: 1991, *Adv. Space Res.* **11**, 1197.
von Rosenvinge, T. T., McDonald, F. B., Trainor, J. H., Van Hollebeke, M. A., and Fisk, L. A.: 1978, *IEEE: Trans.* **GE-16**, 208.
von Steiger, R., Wimmer Schweingruber, R. F., Geiss, J., and Gloeckler, G.: 1995, *Adv. Space Res.* **15** (7), 3.
Wild, J. P., Smerd, S. F., and Weiss, A. A.: 1963, *Ann. Rev. Astron. Astrophys.* **1**, 291.
Yang, J., Turner, M. S., Steigman, G., Schramm, D. N., and Olive, K. A.: 1984, *Astrophys. J.* **281**, 493.